

PULSED POWER SYSTEM OF LINEAR INDUCTION ACCELERATOR FOR FNAL NEUTRINO FACTORY

**V. Kazacha, A. Sidorov (JINR, Dubna, Russia)
I. Terechkine (FNAL)**

1. Introduction

The draft parameters of the FNAL Neutrino Factory (NF) were presented in [1]. A possibility to use an induction linac (LIA) for phase rotation of a muon beam after the target and decay channel was further investigated in [2]. It has been shown that induction linac is capable to provide phase rotation without an additional low-frequency RF-system. Because of the importance of a phase rotation system (PRS) to the NF concept, it was necessary to perform a LIA feasibility study to be sure that the desired pulsed power system can be implemented. Main features of the LIA for the NF phase rotation system are listed below.

1. Before muon beam goes into the Phase Rotation channel, particle's full energy spreads from 170 to 520 MeV [2]. This energy spread is too high to be used in the NF accelerating channel, so it is necessary to reduce it by adjusting the muon beam differential energy and cooling. After the particles are generated in a target, they move through a drift channel to develop a correlation between their energy and position (or time). This correlation makes it possible a phase rotation procedure that means adjustment of particle energy by differential acceleration with the goal to reduce the energy spread. Time-energy correlation calculated in [2] gives us knowledge of a correcting energy that must be added to each portion of the beam to improve its spectrum. It is important that the accelerating voltage pulse shape follows tightly the theoretical correcting energy curve.
2. A large aperture beam channel is required for the muon beam because the beam coming from the target has a very large emittance. The 20-cm aperture for the muon beam is required with magnetic field of 3.0 T. Bore radius of the inductor cores is not less than 40 cm in this case.
3. Duration of the correcting voltage pulse is changing while particles drift in the LIA channel providing an additional mass separation. Starting pulse length of 150 ns was accepted for this study with maximal correcting energy swing of 200 MeV.
4. To avoid an excessive muon loss due to their decay, LIA length must be about 100 m, that results in a change of the accelerating voltage polarity and quite high for the LIA acceleration rate of more than 1 MV/m.
5. The multiple pulse regime (4 pulses within 2 μ sec) has been requested that requires using of a "state-of-art" pulsed power technique.
6. Total muon current does not exceed 100 A. This means that the total system power is mainly defined by induction core power losses.

This note summarizes results of a study made to understand the LIA feasibility and to estimate its major parameters. The main goal was to show that needed pulse shape could be generated using available core materials. After it was understood that the LIA pulse power system can be built, it was necessary to figure out its scale to realize what kind of R&D program is required to approach the system development and design.

The problems of guiding magnetic field forming, core material choice and power losses in a tape-wound core were considered also in [3] and [4]. It was shown in [3] that the problem of fringe field for induction core performance could be simplified by reducing a voltage gap and by shaping a coil profile. A test made at MRTI RAS (Moscow) [5] has shown that a tape-wound core is not sensitive to an axial magnetic field up to 0.03 T level which is enough to consider LIA section layout as it is shown in [3] (see Fig. 1). The section layout shown in this picture was taken as a base for our further study.

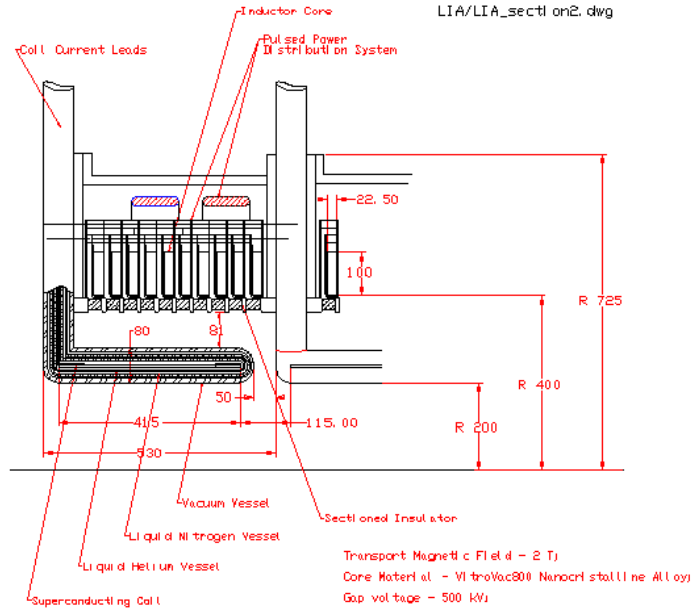


Fig.1: Scheme of accelerating section.

2. Generator Scheme

As it can be seen in [2] (see also Fig. 2 below), correcting voltage pulse at the LIA input is a very non-linear. It was shown in [4] that the required correcting voltage (in MV) per one meter of the LIA length could be fitted by the next expression:

$$U_{th}(t) = -1 + 1.55 \cdot (1 - \exp(\frac{-t}{30 \cdot 10^{-9}})) + 3 \cdot 10^{12} \cdot t \quad (1)$$

The accuracy of this fitting was about 9%. From the point of view of a phase rotation and cooling, it is not very important to have a certain average beam energy gain (or loss). Nevertheless, the differential voltage must be in accordance with the beam energy time distribution found in [2]. Totally about 200 MV of accelerating voltage difference is required to equalize the muon beam energy using phase-rotating LIA. Because "state-of-art" accelerating gradient in LIA is about 1 MV/m, we must consider change of the voltage polarity to be able to keep the LIA length in a range of about 100 m.

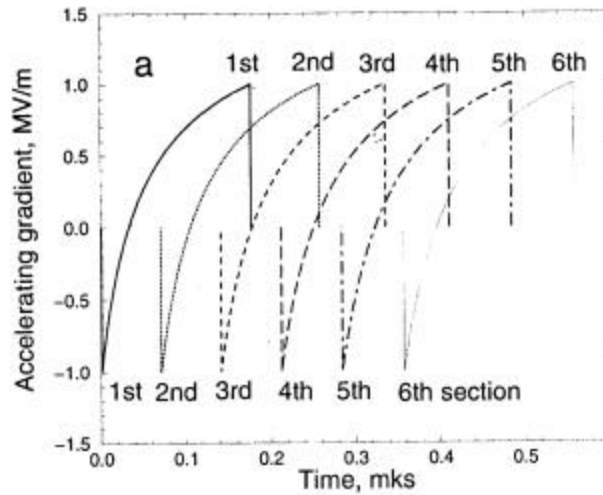


Fig.2: Calculated change of the voltage pulse shape on inductors versus time.

LIA pulse power supply system is to provide a special regime of acceleration and to form the accelerating pulse shape that meets the requirements of the PRS. It is worth to emphasize that it is very important to follow the calculated pulse shape as strictly as it is reasonably possible. It was shown in [4] and proved during this study that from the point of view of energy saving it was desirable to increase decelerating voltage at the expense of accelerating one so that in average the beam is losing its energy. To adjust the working part of the pulse to a needed voltage level and to optimize the PRS LIA parameters, a bias voltage pulse was used.

Core power losses will be discussed in the next section. Here it is necessary to mention that in the generator scheme described below core power loss, which is a nonlinear function of voltage, is represented by a linear resistor. A conceptual scheme of the voltage pulse generator than can generate required voltage pulse is shown in Fig.3.

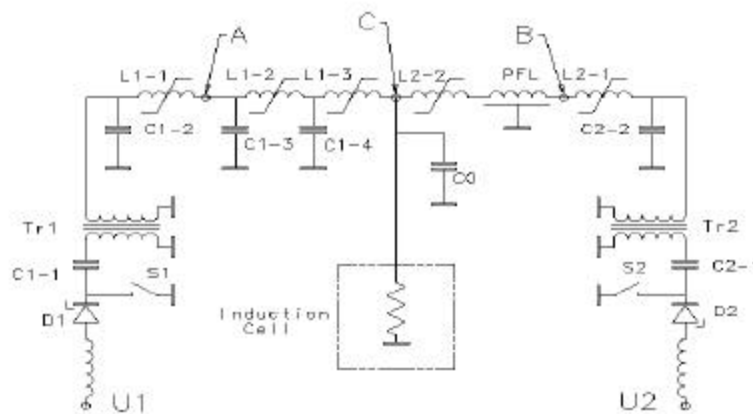


Fig.3: Conceptual scheme of the voltage pulse power generator.

There are two parts in the generator: “charging” part (Fig.3, left from the induction cell) and “forming” part (Fig.3, right from the induction cell). “Charging” part changes voltage of the capacitor C0 to the needed level U_c . The “forming” part of the generator provides output voltage that increases almost exponentially from the level of -1.5 MV up to $+0.5$ MV (per 1 meter of the LIA length). To produce this voltage gain, 20 induction cells are used in each 1-m section, so negative induction core voltage reaches 75 kV. Discharge of the capacitor C0 and pulse forming line (PFL) form working part of the voltage pulse applied to the induction cell. Magnetic switch L2-2 insulates the forming part of the generator when capacitor C0 is being charged. Capacitor C0 is charged to the negative voltage of -95 kV during the first 60 ns by the “charging” part of the generator. To ensure this charge rate, a three-stage magnetic compression circuit is used. The energy to this compression circuit is delivered by the storage capacitor C1-1 through the pulse transformer Tr1. The PFL in the “forming” part of the generator is charged through the single-stage magnetic compression circuit L2-1÷C2-2. The energy for this part of the circuit is stored in C2-1 and Tr2 is used to get needed PFL voltage.

Voltage pulse diagrams produced by the generator are shown in Fig. 4 and Fig. 5.

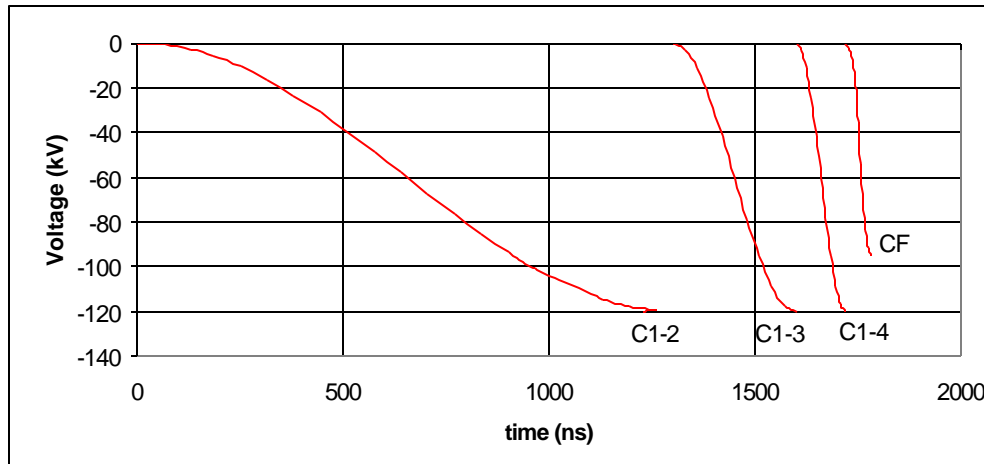


Fig.4: Diagram of voltage pulses for the “charging” part of the generator.

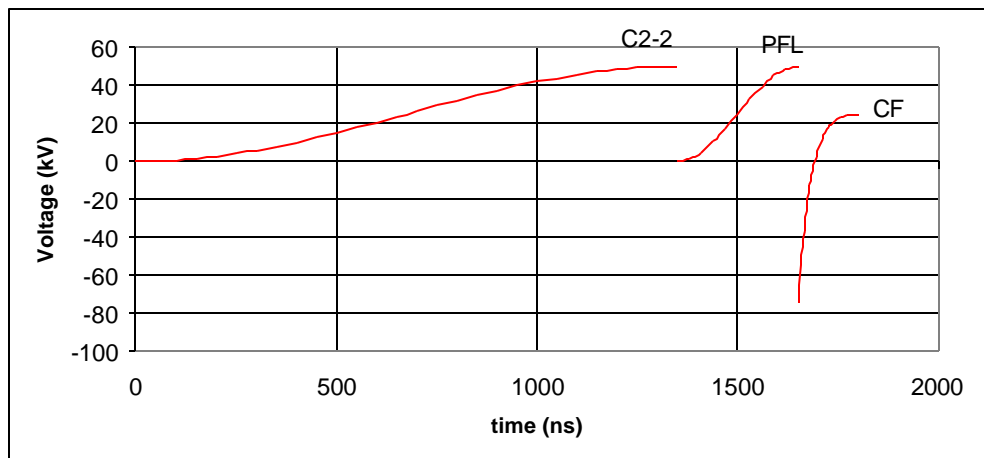


Fig.5: Diagram of voltage pulses for the “forming” part of the generator.

The generator output voltage pulse is shown in Fig. 6.

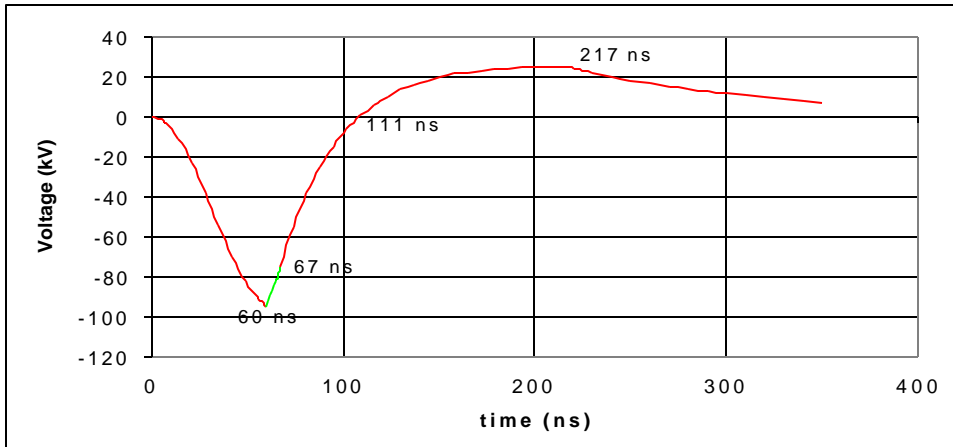


Fig.6: Output voltage pulse applied to an inductor in the LIA section.

During time interval from 0 to 60 ns, the “charging” part of the generator charges the capacitor C0 to the negative voltage -95 kV (see Fig. 6) through the open switch L1-3 (Fig. 3). Starting the moment $t_1=60$ ns, capacitor C0 discharges through the induction cell and back through the switch L1-3. The switch starts to recover, and its resistance increases due to demagnetization of its core. Starting the moment $t_2 = 67$ ns, the switch L2-2 opens, and PFL starts to discharge through the induction cell and into the forming capacitor C0. During the time interval from 67 ns to 111 ns, the voltage on the inductor is negative, magnetic core L1-3 continues to be closed, and its resistance is high enough to neglect energy transfer from the PFL to the capacitor C1-4. When the voltage pulse changes its polarity, switch L1-3 stays closed until volt-seconds of the positive part of the pulse (from 111 ns till 217 ns) become larger than volt-seconds of the negative part of the pulse (from 60 ns till 111 ns). That's why to support the long positive tail of the required pulse shape, it is desirable to have higher negative voltage at the very beginning of the active part of the pulse: it helps to reduce the duration of the capacitor C0 discharge period (from 60 ns to 67 ns).

As it is shown in Fig. 6, during the active part of the pulse that is used for phase rotation, inductor voltage changes from -75 kV up to $+25$ kV. For 1-m accelerating section, voltage changes from -1.5 MV in the beginning of the active part of the voltage pulse up to $+0.5$ MV in the end. Time duration of the negative and the positive parts of the voltage pulse (not only of the active part of the pulse) are chosen so that their volt-second areas are equal to each other. As a result, magnetic recovery of the induction cell core is reached automatically, and after one voltage pulse ends, the system is ready to accept the next one. The next pulse can start immediately after the previous one.

Impedance of the circuit described above can not be made arbitrarily small. Nevertheless, it appears possible to use one generator to feed 10 inductors (0.5-m length) in parallel.

The four-pulse regime can be realized using the generator, which scheme is shown in Fig. 7. Both “charging” and “forming” parts of the generator contain four primary circuits. Each primary circuit acts once during $2 \mu\text{s}$ so that four voltage pulses are generated. Each primary circuit in the “charging” part of the generator is separated from

the rest three circuits by nonlinear reactors L1-1 ÷ L1-4 (magnetic switches). In order to avoid energy transfer into unused primaries, the reactors' volt-second areas were chosen to be by a factor of 3 greater than the volt-second areas of the magnetic switches L1-5 and L1-6 taken together. The same logic was used to choose parameters of the reactors L2-1 ÷ L2-4 of the "forming" part of the generator.

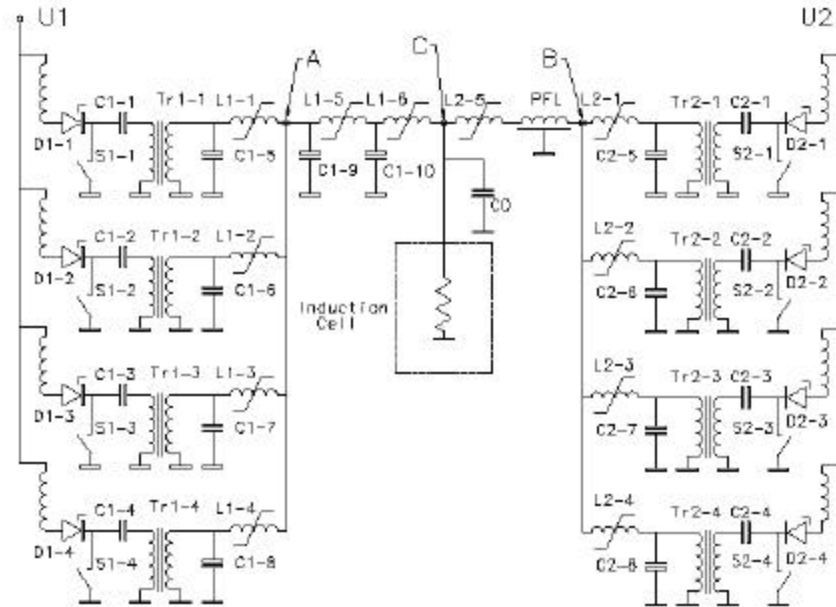


Fig.7: Principal scheme of the LIA pulse generator.

The main parameters of the capacitors, transformers and magnetic switches for both generators are presented in tables 1÷6. The generator is capable to feed 10 inductors (0.5 m) and requires 24 kW of average power from the network (or 4.8 MW per 100 m).

Table 1. Reactors for the "charging" part of generator

Reactor	L1-(1÷4)	L1-(1÷4)	L1-5	L1-6	L1-6
Material	Metglas 2605SC	Vitrovac 7600	Metglas 2705MN	Vitrovac 6150	Metglas 2705MN
Satur. Ind. (nH)	<563	<563	<98	<27	<27
Volt-seconds (V·s)	$78 \cdot 10^{-3}$	$78 \cdot 10^{-3}$	$18 \cdot 10^{-3}$	$7.2 \cdot 10^{-3}$	$7.2 \cdot 10^{-3}$
Cross-section (cm ²)	192	169	112	18	15
Volume (cm ³)	9660	7974	2×3672	10×622	10×554
Number of turns	2	2	1	3	3
Amount of reactors	1	1	2	10	10

Table 2. Capacitors for the “charging” part of generator

	C1-(1÷4)	C1-(5÷8)	C1-9	C1-10	C _F
Capacitance (nF)	310	34	31	28.3	26

Table 3. Pulse transformer for the “charging” part of generator

	Ratio	U _{second} (kV)	S (cm ²)	V (cm ³)
Metglas 2605SC	1:3	120	25	1200
Vitrovac 7600	1:3	120	21.2	952

Table 5. Reactors for the “forming” part of generator

Reactors	L2-(1÷4)	L2-(1÷4)	L2-5	L2-5
Material	Vitrovac 7600	Metglas 2605SC	Vitrovac 6150	Metglas 2705MN
Satur. Ind. (nH)	<348	<348	<123	<123
Volt-seconds (V·s)	32.4 10 ⁻³	32.4 10 ⁻³	10.45 10 ⁻³	10.45 10 ⁻³
Cross-section (cm ²)	48	80	7.9	8
Volume (cm ³)	1810	2010	10×302	10×235
Number of turns	3	2	10	10
Amount of reactors	1	1	10	10

Table 4. Capacitors for the “forming” part of generator

	C2-(1÷4)	C2-(5÷8)	C _{PFL}
Capacitance (nF)	200	50	~ 47

Table 6. Pulse transformers for the “forming” part of generator

Material	Ratio	U _{second} (kV)	S (cm ²)	V (cm ³)
Metglas 2605SC	1:2	120	16	603
Vitrovac 7600	1:2	120	14	506

3. Induction Core

The key issue for developing a pulsed power system for a LIA is power loss in an induction core. Knowledge of how power loss in a core depends on core magnetization rate and excitation field allows us to make a realistic estimate of a power, required to operate the phase rotation LIA with its unique voltage pulse shape. The model that describes energy losses for a core made of a ferromagnetic metal ribbon was developed by Carl H. Smith [6]. Depending of core magnetization rate, different processes are responsible for loss of energy. In our analysis, we accept that magnetization rate is very

high and magnetic domain wall movement mechanism is responsible for the major part of power losses in a core. For example, for nanocrystalline alloy FT-1H, at magnetization rate of more than 10 T/μs, eddy currents described in terms of saturation wall domain movement explain about 95% of total core power loss. Following [6], we can write for the magnetic field $H(t)$ driving the saturation wave domain movement:

$$H(t) = \left(\frac{d^2}{4r} \right) \cdot \left(\frac{\Delta B(t)}{2B_s} \right) \cdot \left(\frac{dB}{dt} \right) \quad (2)$$

where $\Delta B(t) = B(t) - B_r$ is an efficient flux density swing, B_s is material saturation field, B_r is residual field, d is ribbon thickness, and r is a specific material resistance (all dimensions are in accordance with SI).

Power loss per unit of a magnetic material volume is described by the expression:

$$p(t) = H(t) \cdot \frac{dB(t)}{dt}, \quad (3)$$

that gives after using (2) [5]

$$p(t) = \left(\frac{d^2}{4r} \right) \cdot \left(\frac{B(t) + B_r}{2B_s} \right) \cdot \left(\frac{dB}{dt} \right)^2 \quad (4)$$

We can find $\frac{dB}{dt}$ if we know required voltage pulse shape $U(t)$:

$$\frac{dB}{dt} = \frac{U(t)}{S}, \quad (5)$$

where S is an effective core cross-section per one meter of LIA length. To calculate the power necessary to support this voltage, mathematical description of the LIA cell voltage pulse shown in Fig. 6 was made based on the generator scheme in Fig. 3. As one can see from Fig. 8, if scheme parameters are chosen properly, the working part of the inductor voltage pulse follows closely the required correction voltage curve expressed by (1).

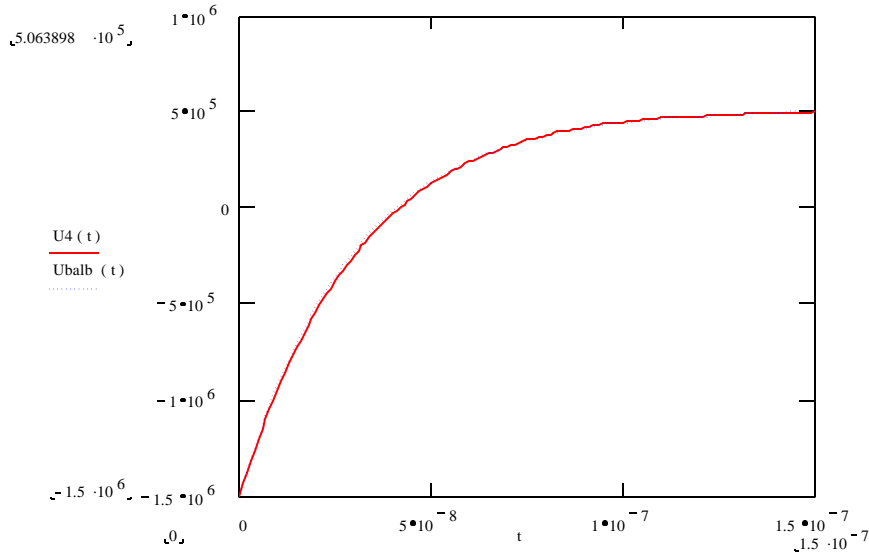


Fig.8: Generator output voltage (adjusted to 1-m LIA section) - solid line and required section correcting voltage fitted by (1) - dotted curve.

For given B_s we can find minimal cross section area of a core S_{\min} as

$$S_{\min} \approx \frac{Q_{neg}}{2B_s}, \quad (6)$$

where Q_{neg} is area of the negative part of the voltage pulse. As an example, Fig.9 shows calculated magnetic flux density B [T] in a core versus time for the case when $B_r = 1.1$ T, $B_s = 1.2$ T, $d = 25 \cdot 10^{-6}$ m, and $\rho = 1.35 \cdot 10^{-6}$ Ohm m.

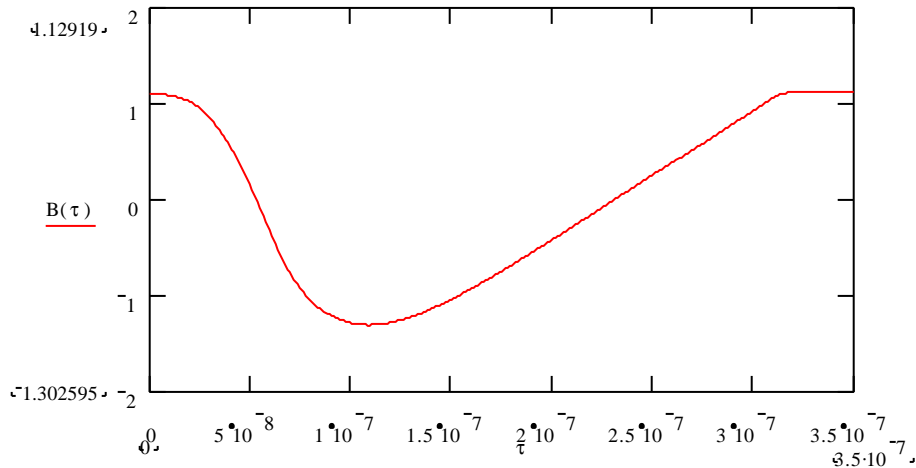


Fig.9: Magnetic flux density in an induction cell core during magnetization cycle

Instant power loss $P(t)$ [W] per 1 meter of the LIA length calculated with the help of formulae (4) and (5) for the same core parameters is shown in Fig.10.

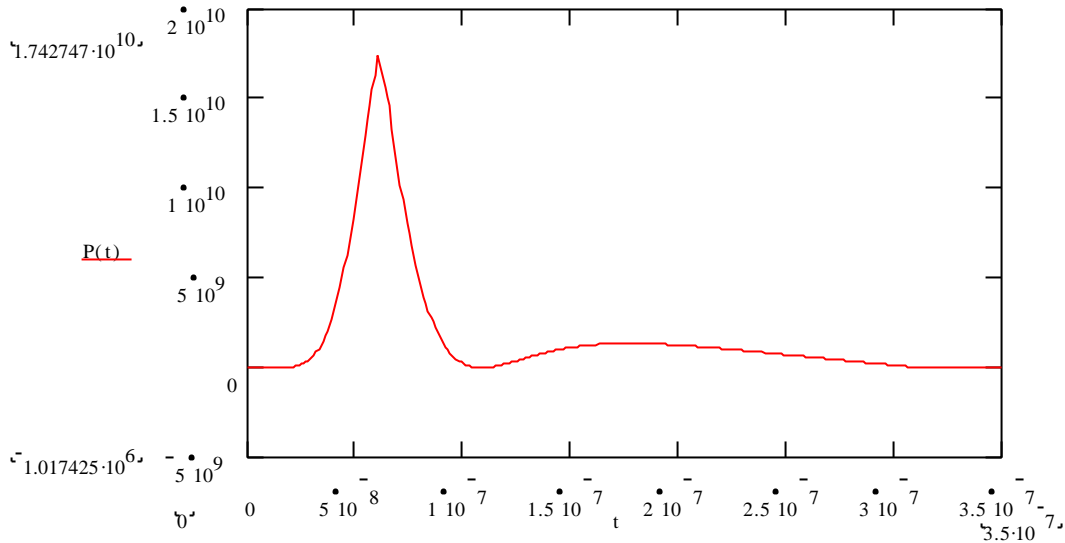


Fig.10: Calculated instant power loss per 1 meter of LIA length

Total core energy loss can be found by integrating instant loss over time. Table 7 summarizes calculations of LIA core power loss. Two types of ferromagnetic materials were used: V6150 and Metglas 2705MN. In this table W is full energy loss in inductor cores per 1 meter per 1 pulse; P_{\max} is peak power loss; P_{av} is averaged power loss per

100-m IIA length for the four-pulse regime and 15 Hz operation frequency. Total LIA induction cell core mass M is shown in the last column of the table. Specific weight for both ferromagnetics was accepted to be 7.3 g/cm^3 . Two materials were used to calculate core parameters in the table: alloy V6150 ($B_r = 0.9 \text{ T}$, $B_s = 1.0 \text{ T}$) and Metglas 2705MN ($B_r = 1.1 \text{ T}$, $B_s = 1.2 \text{ T}$).

Table 7. LIA core parameters and power loss summary

	$S_{\min} \text{ (m}^2\text{/m)}$	$W \text{ (J/m)}$	$P_{\max} \text{ (GW/m)}$	$P_{\text{av}} \text{ (MW)}$	$M \text{ (Ton)}$
V6150	0.045	514	14.7	3.1	94
2705MN	0.037	612	17.4	3.7	78

It is necessary to mention that the parameters in the table above were found using the smallest core cross-section that withstands required volt-seconds. According to [4], a significant gain in energy loss is expected if we increase this cross-section. Using tables 1÷6, it is possible to find the weight and the volume of LIA pulsed power system equipment. For each 1-m LIA section, about 4 m^3 of equipment is needed. This equipment can be installed in the vicinity of the LIA section it is feeding using two-layer layout, as it is shown in the picture in Fig. 11.

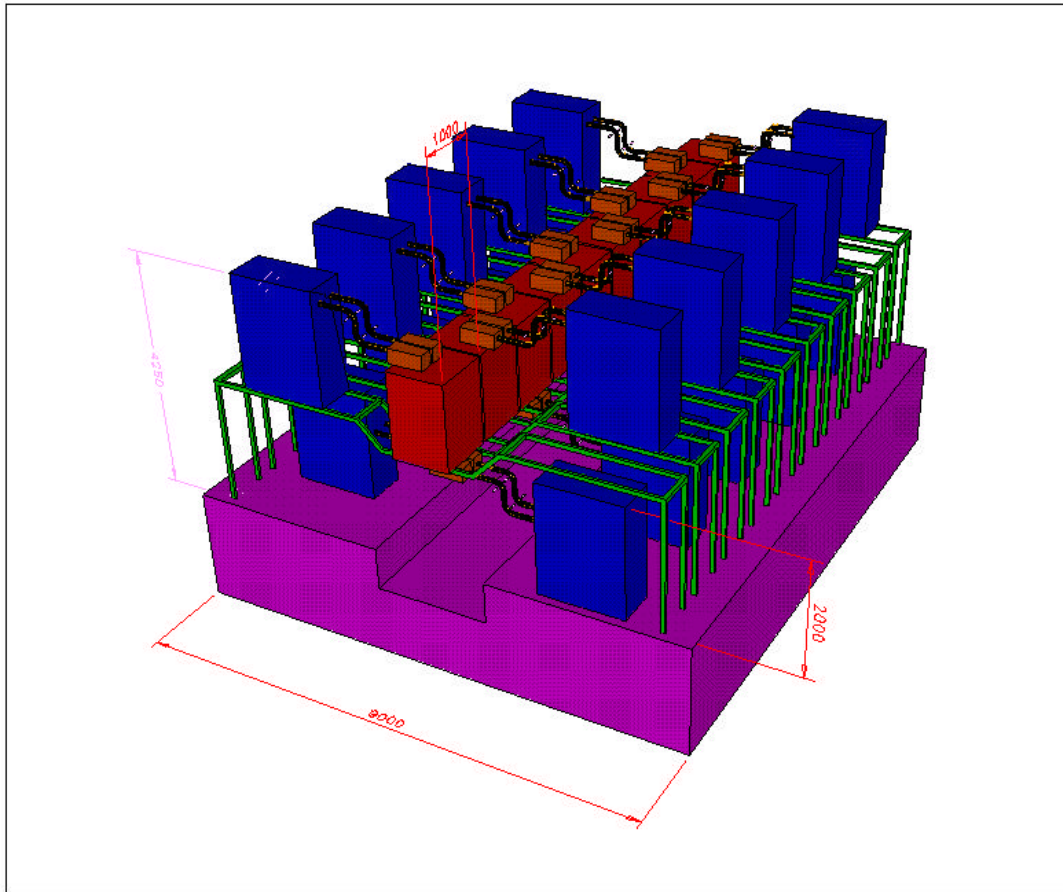


Fig. 11. Possible layout of the LIA pulsed power system

Vacuum system, cryogenic equipment and primary energy supplies are not shown here. It is necessary to mention one more time that the layout shown corresponds to the system that was not finally optimized to reduce its volume (and cost). It should be done during the stage of R&D. Other tasks for the R&D program are listed below

4. Suggested R&D Program

The study conducted has shown that the idea of using LIA for muon beam phase rotation does not have obvious reasons to be rejected at this stage. More over, LIA parameters look quite realistic, and its implementation does not require using a technique that was not tried yet. Nevertheless, to fully realize technical problems that can arise during LIA construction and testing, an R&D program must start that includes:

- LIA pulse power scheme optimization with the goal to reduce maximal power;
- Pulsed power scheme modeling using a specialized software taking into account nonlinear behavior of the pulse power system element;
- Pulse power scheme development for different pulse lengths corresponding to different locations of an accelerating section in the LIA;
- Modeling of performance of a core exposed to axial magnetic field;
- Development, design, fabrication and testing of a full scale LIA module including accelerating section, magnetic system, and pulse generator.

5. Conclusion

1. Pulsed power system for the NF LIA has been developed that allows forming the accelerating voltage pulse with required shape.
2. The first order evaluation of the induction system was made that has provided us with a set of major LIA parameters:
 - induction cell core minimal cross-section area is $18.5 \div 22.5 \text{ cm}^2$ (without taking into account its space factor);
 - induction cell core volume is $5000 \div 6000 \text{ cm}^3$;
 - tape-wound induction core volume for the total LIA is $10 \text{ m}^3 \div 12 \text{ m}^3$;
 - tape-wound induction core weight for the total LIA is $73 \div 88 \text{ Ton}$;
 - average LIA power consumption is to 4.8 MW (only for the pulsed power system).
3. The next step of the LIA development must include thorough pulsed power circuit simulation that takes into account nonlinear induction cell impedance, stray inductance, and stray capacitance of section constructive elements.

REFERENCES

1. R.B. Palmer, Neutrino Factory Draft Parameters, www-mucool.fnal.gov/mcnotes/muc0046.ps. 1999.
2. V. Balbekov, Phase Rotation with Induction Linac, www.tdpc02.fnal.gov/terechki/LIA/Balbekov
3. I Terechkine, LIA for the Neutrino Factory at FNAL, http://www.fnal.gov/project/moun_collider/nu_factory/subsys/ss-phrot/nuss-phr

March 8, 2000

4. I. Terechkine, Neutrino Factory Phase-Rotation LIA: Pulsed Power System Optimization,
http://www.fnal.gov/project/moun_collider/nu_factory/subsys/ss-phrot/nuss-phr
5. S.L. Mamaev, S.L. Puchkov, G.L. Mamaev, LIA Core Magnetization in Fringe Magnetic Field. Summary of the test made at MRTI (Moscow, Russia) in support of Phase Rotation LIA studies. Interpreted by Yu. Terechkine,
http://www.fnal.gov/project/moun_collider/nu_factory/subsys/ss-phrot/nuss-phr
6. Carl H. Smith, Application of amorphous magnetic materials at very-high magnetization rates, *J.Appl. Phys.* 67 (9), 1990, pp. 5556 – 5561.